Neuron, Volume *99*

Supplemental Information

Mouse Motor Cortex Coordinates the Behavioral Response to Unpredicted Sensory Feedback

Matthias Heindorf, Silvia Arber, and Georg B. Keller

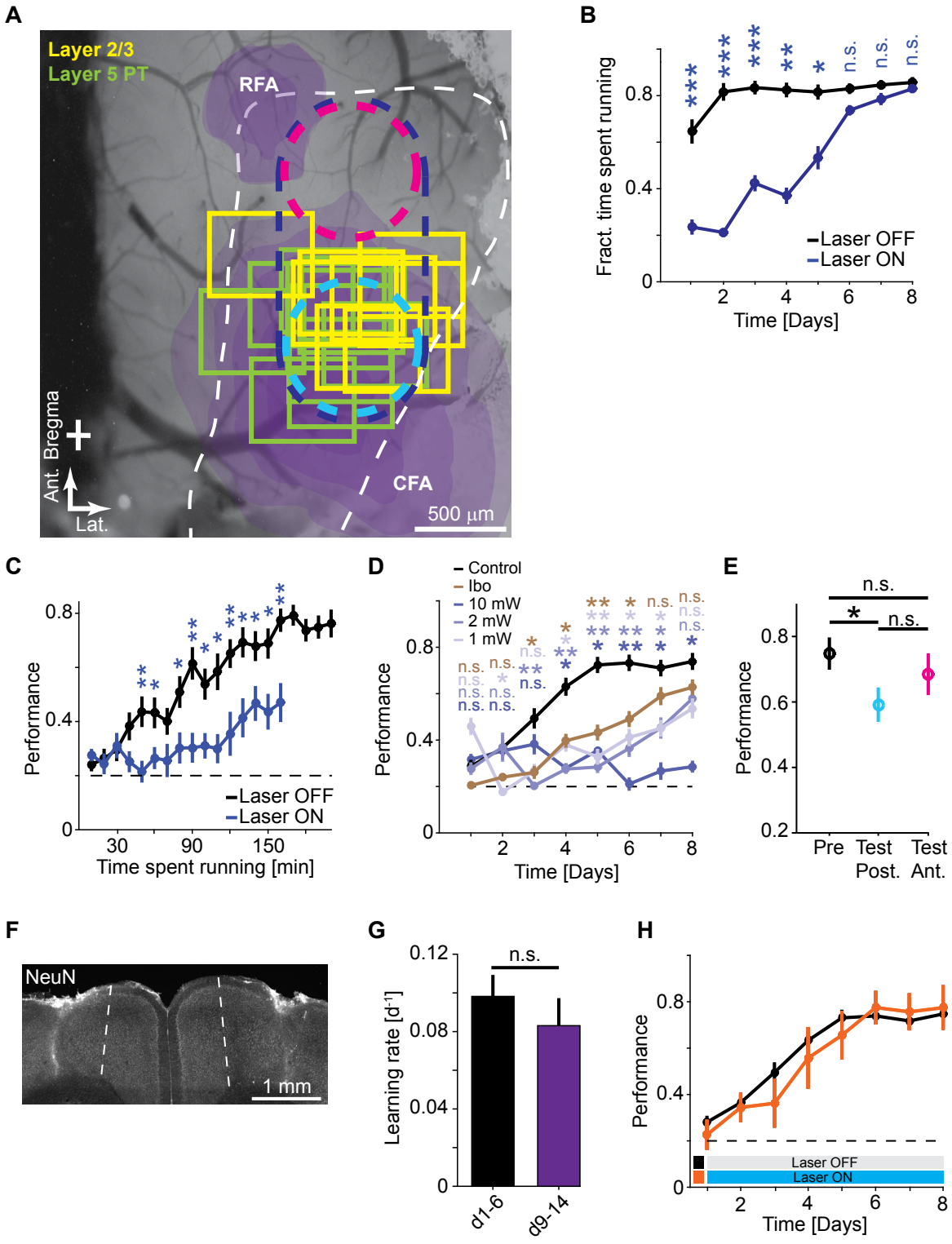
A
Layer 2/3
Layer 5 PT
RFA
CFA
Ant.
Bregma
Lat.
500 µm
B
Fract. time spent running
Time [Days]
Laser OFF
Laser ON
C
Performance
Time spent running [min]
Laser OFF
Laser ON
D
Control
Ibo
10 mW
2 mW
1 mW
Performance
Time [Days]
E
Performance
Pre
Test Post.
Test Ant.
F
NeuN
1 mm
G
Learning rate [d-1]
d1-6
d9-14
H
Performance
Time [Days]
Laser OFF
Laser ON

Figure S1. Inhibition of CFA reduces task performance – additional information and controls. Related to Figure 1.

(**A**) Approximate location of the imaging fields of view (550 µm x 450 µm) in layer 2/3 (yellow, n = 8 mice) and layer 5 PT (green, n = 11 mice) experiments superimposed on an example wide-field fluorescence image of motor cortex. Dashed dark blue oval marks full-width half maximum of the laser beam at the surface of cortex (10 mW average power per hemisphere, see STAR Methods) at the endpoints of the scan during optogenetics experiments. Purple shading marks the caudal forelimb area (CFA) and the rostral forelimb area (RFA) in motor cortex (dashed white line); adapted from (Tennant et al., 2011). Dashed blue and pink circles mark optogenetic stimulation locations for inhibition experiments targeted at the CFA or a more anterior region in motor cortex, at 1 mW and 2 mW average power per hemisphere. Ant.: anterior; Lat.: lateral; white cross marks bregma.

(**B**) Fraction of time spent running without (black, n = 22 mice) and with (blue, n = 12 mice) bilateral inhibition of motor cortex as a function of training days. Fraction of time spent running was higher without inhibition of motor cortex. Error bars indicate SEM over mice. n.s.: not significant, *: $p < 0.05$, **: $p < 0.01$, ***: $p < 10^{-3}$; Wilcoxon rank sum test between groups.

(**C**) Performance as a function of time spent running for the first 8 days of training. Same coloring as in **B**. Error bars indicate SEM over mice. Dashed black line marks chance performance. *: $p < 0.05$, **: $p < 0.01$; Wilcoxon rank sum test between groups.

(**D**) Quantification of the average performance as a function of training days, laser power and stimulus location (as outlined in **A**, see STAR Methods) in mice with (dark blue, rostral and caudal location, 10 mW, n = 3 mice; intermediate blue, caudal location, 2 mW, n = 5 mice; pale blue, caudal location, 1 mW, n = 4 mice) or without (black, n = 22 mice) motor cortex inhibition or chronic ibotenic acid micro-lesions (Ibo, brown, n = 5 mice). Note that using lower laser power centered on the CFA still significantly impaired learning. Dashed black line marks chance performance. n.s.: not significant, *: $p < 0.05$, **: $p < 0.01$; Wilcoxon rank sum test vs control group.

(**E**) The effect of decrease in performance in expert mice was larger when optogenetically inhibiting the posterior location (CFA, cyan) than when inhibiting the anterior location (pink). Error bars indicate SEM over mice (n = 9 mice). *: $p < 0.05$, n.s.: not significant; Wilcoxon rank sum test.

(**F**) Confocal image of a bilateral chronic ibotenic acid micro-lesion of the CFA in a *C57/Bl6* mouse. Coronal slice is 0.5 mm anterior or bregma. Dashed lines mark medial CFA boundaries.

(**G**) Learning rate in **Figure 1C** days 1 to 6 for mice without inhibition of motor cortex (black, n = 22 mice) and days 9 to 14 for mice with bilateral inhibition of motor cortex (purple, n = 3 mice). Error bars indicate SEM over mice. n.s.: not significant; $p = 0.42$; Wilcoxon rank sum test.

(**H**) Performance of *C57BL/6* mice that received blue laser stimulation in motor cortex during training, but did not express channelrhodopsin-2 in vGAT+ interneurons (n = 4 mice, orange line), compared to mice that were trained without blue laser (n = 22 mice, black line). Error bars indicate SEM over mice. Dashed black line marks chance performance.

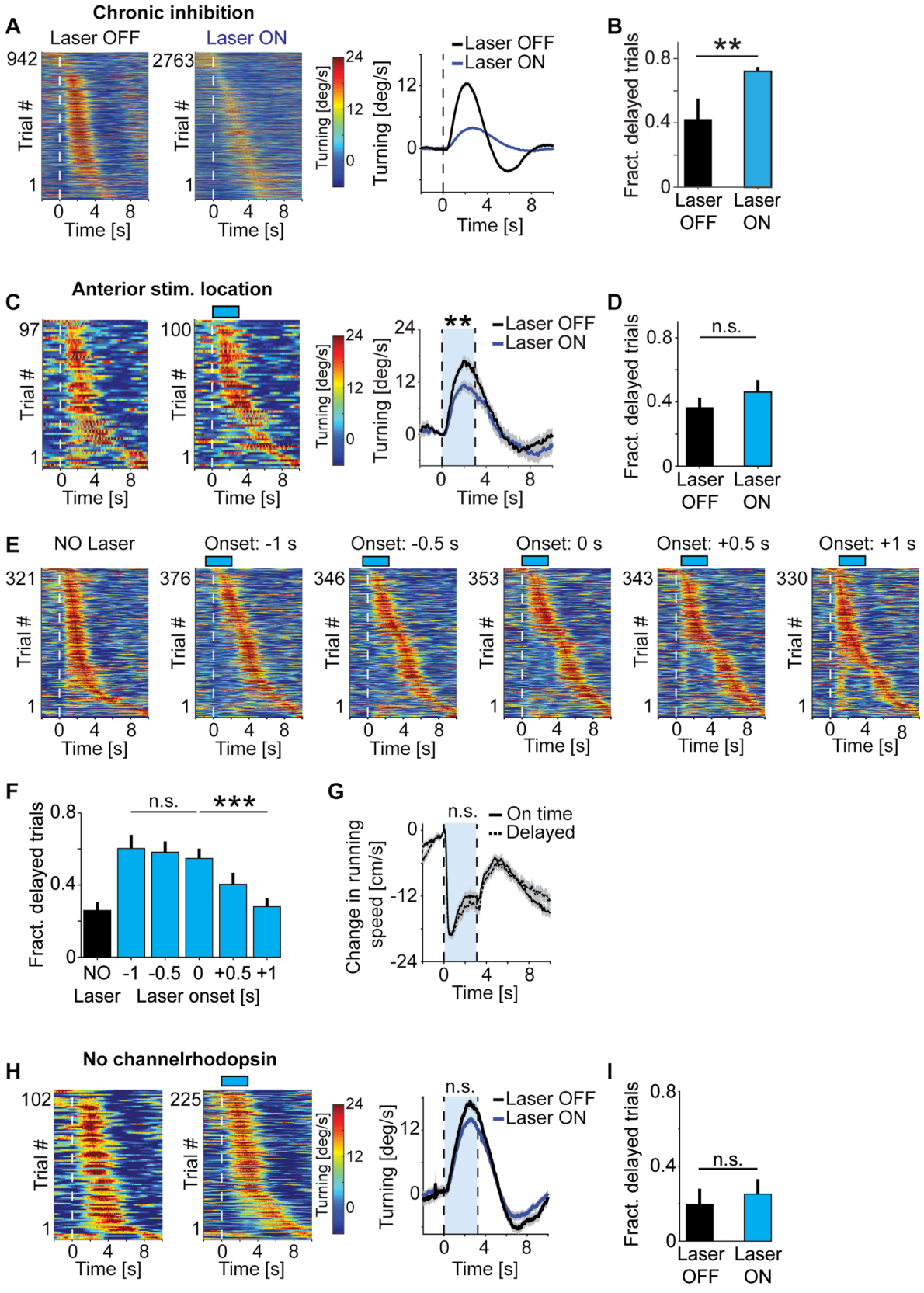
A
Chronic inhibition
Laser OFF
Laser ON
942
2763
Trial #
Time [s]
Turning [deg/s]
Laser OFF
Laser ON
B
Fract. delayed trials
**
Laser OFF
Laser ON
C
Anterior stim. location
97
100
**
D
n.s.
E
NO Laser
Onset: -1 s
Onset: -0.5 s
Onset: 0 s
Onset: +0.5 s
Onset: +1 s
321
376
346
353
343
330
F
n.s.
***
NO Laser
-1
-0.5
0
+0.5
+1
Laser onset [s]
G
n.s.
On time
Delayed
Change in running speed [cm/s]
H
No channelrhodopsin
102
225
I
n.s.

Figure S2. Channelrhodopsin-2 mediates impairment during photoinhibition. Related to Figure 2.

(**A**) Responses to visual offset perturbations were greatly reduced during chronic bilateral inhibition of motor cortex. Left panel: Turning velocity response to 942 visual offset perturbations in 3 mice during training days 3 to 8 without chronic inhibition of motor cortex, sorted by time to peak velocity. Middle panel: Turning velocity response to 2763 visual offset perturbations in 12 mice (data from all three inhibition power levels 1 mW, 2 mW, and 10 mW combined) during training days 3 to 8 with chronic bilateral inhibition of motor cortex, sorted by time to peak velocity. Color indicates turning speed. Right panel: Average speed profile for the data shown in left and middle panels. Shading indicates SEM over turns.

(**B**) Fraction of delayed turns (see STAR Methods) without (left, black) or with (right, cyan) chronic photoinhibition. Same data as in **A**. Error bars indicate SEM over mice. **: $p < 0.01$; Wilcoxon rank sum test.

(**C**) Speed profile of 97 visual offset perturbation-induced corrective turns in expert mice that had reached plateau performance without (left panel, n = 9 mice) and with (middle panel, 100 trials, n = 9 mice) bilateral inhibition of anterior motor cortex (pink circle in **Figure S1A**) concurrent with visual offset perturbation for 3 s (blue bar). Turns are sorted by latency to peak velocity. Right panel: Average speed profile for the data shown in left and middle panels. Shading indicates SEM over turns. **: $p < 0.01$; Wilcoxon rank sum test.

(**D**) Fraction of delayed turns (see STAR Methods) without (left, black) photoinhibition or with (right, cyan) photoinhibition concurrent with visual offset perturbation. Same data as in **C**. Error bars indicate SEM over mice (n = 9 mice). n.s.: not significant; Wilcoxon rank sum test.

(**E**) Turning responses to visual offset perturbations during different inhibition onset times relative to visual offset perturbation, sorted by time to peak velocity. Data were collected in expert mice that had received at least 8 training sessions. Stimulation onset and duration indicated by blue bar. Color indicates turning speed as in **A**.

(**F**) Fraction of delayed turns (see STAR Methods) as a function of the timing of laser inhibition onset relative to the visual offset perturbation (data from all three inhibition power levels 1 mW, 2 mW, and 10 mW combined). Error bars indicate SEM over mice (n = 14 mice). ***: $p < 10^{-3}$, n.s.: not significant; Wilcoxon rank sum test.

(**G**) Reduction of running speed induced by concurrent inhibition of motor cortex and visual offset perturbation for trials in which mice executed an induced turn on time (solid black line, n = 144) and for trials in which mice delayed the induced turn until the offset of the inhibition of motor cortex (dashed black line, n = 209). Trials are same as in **E**, 0 s onset. Blue bar marks duration of motor cortex inhibition (0 s to 3 s). Shading indicates SEM over trials. n.s.: not significant; Wilcoxon rank sum test.

(**H**) Speed profile of visual offset perturbation-induced corrective turns in mice that did not express channelrhodopsin-2 in vGAT+ interneurons without (left panel, 102 turns, n = 5 mice) and with (middle panel, 225 turns, n = 5 mice) blue laser stimulation of motor cortex concurrent with visual offset perturbation for 3 s (blue bar). Data are from expert mice with at least 8 training sessions. Trials are sorted by latency to peak turning velocity. Color indicates turning speed. Right panel: Average speed profile for the data shown in left and middle panels. Shading indicates SEM over turns. n.s.: not significant; Wilcoxon rank sum test.

(**I**) Fraction of delayed turns (see STAR Methods) in mice (n = 5 mice) that did not express channelrhodopsin-2 in vGAT+ interneurons without (black) or with blue laser stimulation of motor cortex concurrent with visual offset perturbation (blue). Error bars indicate SEM over mice. n.s.: not significant; Wilcoxon rank sum test.

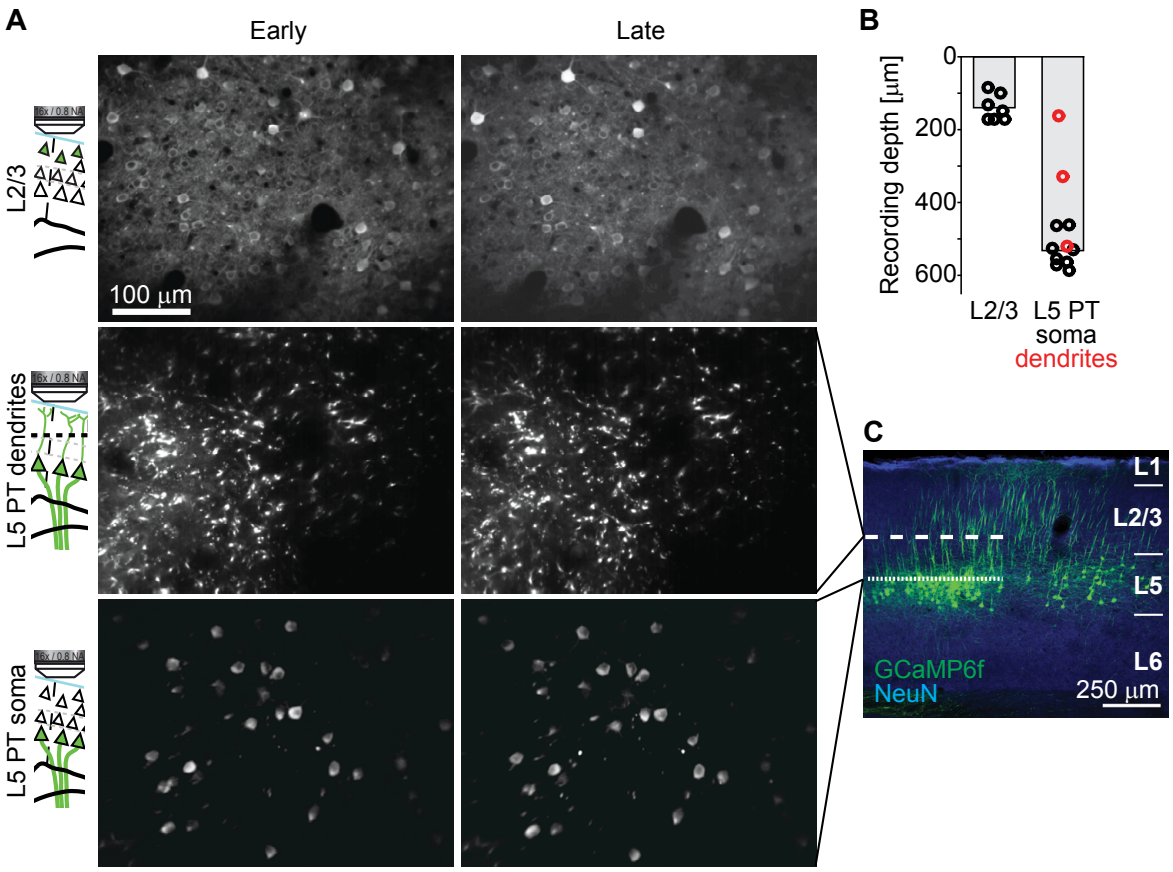
A
Early
Late
L2/3
L5 PT dendrites
L5 PT soma
100 µm
B
Recording depth [µm]
0
200
400
600
L2/3
L5 PT soma
dendrites
C
L1
L2/3
L5
L6
GCaMP6f
NeuN
250 µm

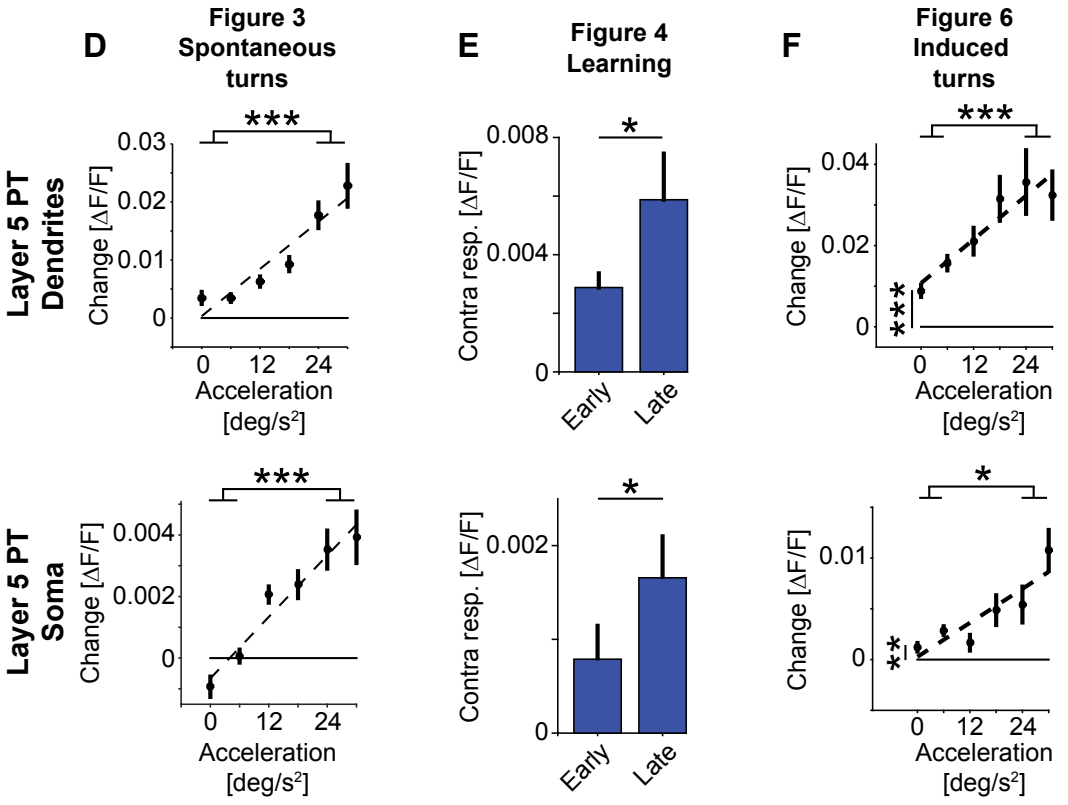
Figure 3
Spontaneous turns
Figure 4
Learning
Figure 6
Induced turns
D
E
F
Layer 5 PT Dendrites
Layer 5 PT Soma
Change [ΔF/F]
Contra resp. [ΔF/F]
Acceleration [deg/s²]
Early
Late
***
*
**

Figure S3. Data recorded from layer 5 PT dendrites and layer 5 PT soma are qualitatively comparable. Related to Figure 3.

(**A**) Sample two-photon maximum projections of the same layer 2/3 (top row), layer 5 PT soma (middle row) and layer 5 PT dendrite recordings early (left column) and late (right column) in the course of training.

(**B**) Depth of recording below the pial surface of cortex for the layer 2/3 recordings and the layer 5 PT recordings. Each dot corresponds to one imaging site. In red are the recording sites in which we imaged dendrites of layer 5 PT neurons because imaging quality at the somata was not sufficient for data analysis.

(**C**) Confocal image of layer 5 PT neurons in motor cortex of a *Sim1(KJ18)-Cre* mouse injected with AAV2/1-EF1α-DIO-GCaMP6f. White dashed line and white dotted line indicate approximate locations of layer 5 PT dendrites and layer 5 PT soma recordings, respectively, as shown in **A**.

(**D**) Comparison of the scaling of the response with acceleration of spontaneous turns (as in **Figure 3J**) in dendrites and somata separately. Error bars indicate SEM over the number of compartments. ***: $p < 10^{-3}$, n = 224 somata and 336 dendrites; paired Student's t test.

(**E**) Comparison of the increase of neuronal activity in response to contraversive turns (as in **Figure 4E**) in dendrites and somata separately. Error bars indicate SEM over the number of compartments. *: $p < 0.05$, n = 224 somata and 336 dendrites; paired Student's t test.

(**F**) Comparison of the scaling of the response with acceleration of induced turns (as in **Figure 6F**) in dendrites and somata separately. Error bars indicate SEM over the number of compartments. *: $p < 0.05$, ***: $p < 10^{-3}$, n = 224 somata and 336 dendrites; paired Student's t test.

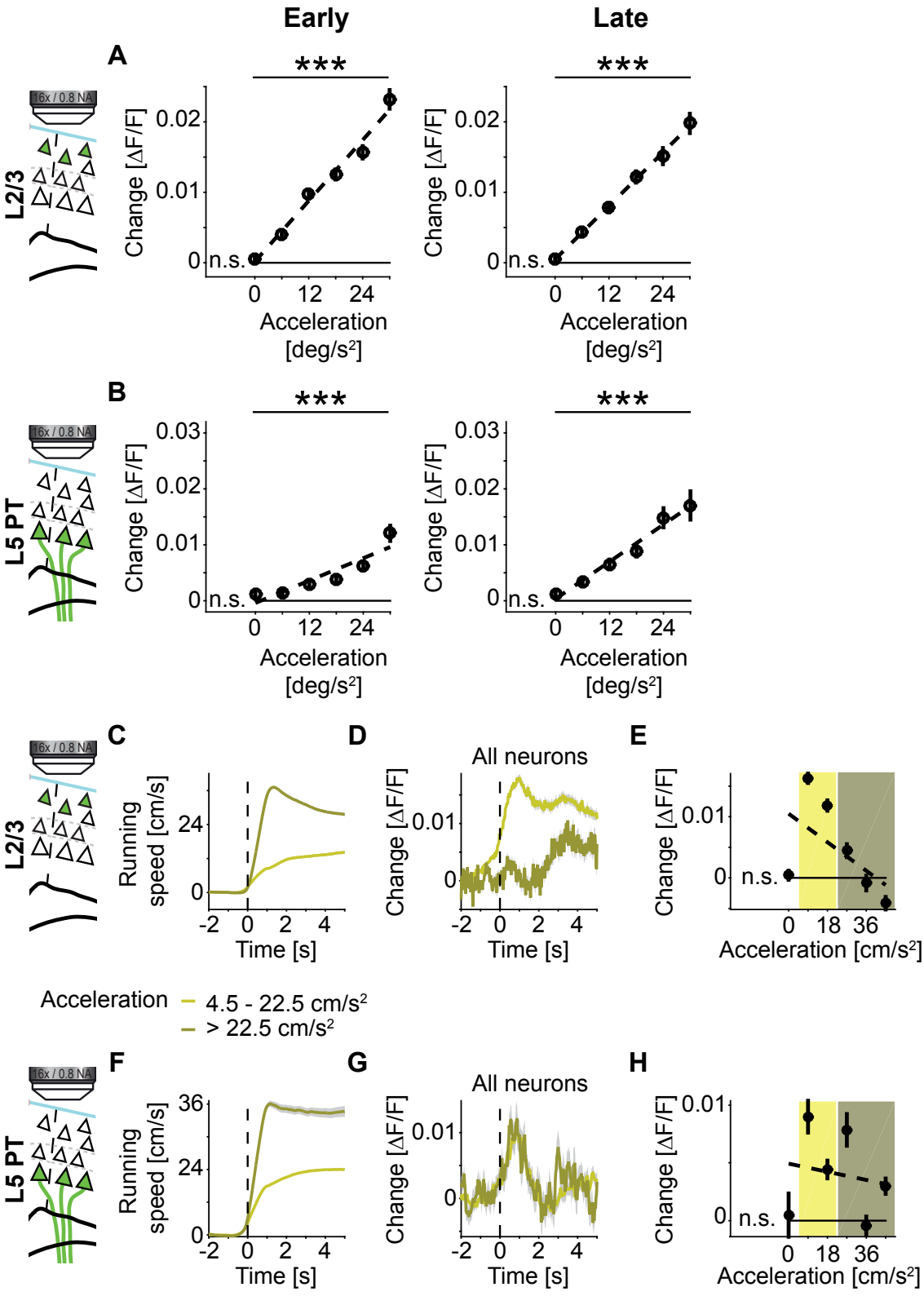
Early
Late
A
***
***
16x / 0.8 NA
L2/3
Change [ΔF/F]
0.02
0.01
0
n.s.
0
12
24
Acceleration
[deg/s²]
B
***
***
16x / 0.8 NA
L5 PT
Change [ΔF/F]
0.03
0.02
0.01
0
n.s.
0
12
24
Acceleration
[deg/s²]
C
D
E
16x / 0.8 NA
L2/3
Running
speed [cm/s]
24
0
-2
0
2
4
Time [s]
All neurons
Change [ΔF/F]
0.01
0
-2
0
2
4
Time [s]
Change [ΔF/F]
0.01
0
n.s.
0
18
36
Acceleration [cm/s²]
Acceleration
4.5 - 22.5 cm/s²
> 22.5 cm/s²
F
G
H
16x / 0.8 NA
L5 PT
Running
speed [cm/s]
36
24
0
-2
0
2
4
Time [s]
All neurons
Change [ΔF/F]
0.01
0
-2
0
2
4
Time [s]
Change [ΔF/F]
0.01
0
n.s.
0
18
36
Acceleration [cm/s²]

Figure S4. Activity scales linearly with spontaneous turn amplitude in both early and late phases of training, but not with acceleration during running initiation. Related to Figure 3.

(**A**) Activity of layer 2/3 neurons scales linearly with the acceleration of the turn both early (days 1 to 4, left) and late (days 5 to 8, right) in training. Error bars indicate SEM over neurons (n = 1154 neurons). ***: $p < 10^{-3}$, early: $R^2 = 0.07$, late: $R^2 = 0.04$, n = 1154 neurons; linear trend analysis (see STAR Methods). n.s.: not significant; Student's t test.

(**B**) Same as **A**, but for layer 5 PT neurons (n = 560 neurons). Early: $R^2 = 0.05$, late: $R^2 = 0.03$, n = 560 neurons; linear trend analysis (see STAR Methods).

(**C**) We split running onsets detected throughout training (days 1 to 8) into bins of high (dark yellow) and low (light yellow) acceleration. Shading indicates SEM over running onsets (number of high acceleration onsets: n = 901; low acceleration onsets: n = 1485).

(**D**) Average population activity of layer 2/3 neurons for the running onsets shown in **C** (n = 1154 neurons). Using the same binning as in **C**, the average neuronal activity was higher during running onsets of low acceleration. Colors as in **C**. Shading indicates SEM over neurons.

(**E**) Average population activity for layer 2/3 neurons (n = 1154 neurons) as a function of acceleration of the running onset. Error bars indicate SEM over neurons. Dashed black line is a linear fit to the data. n.s.: not significant, lowest bin is not different from zero; Student's t test.

(**F**) As in **C**, but for the layer 5 PT experiments (number of high acceleration onsets: n = 131; low acceleration onsets: n = 1914).

(**G**) As in **D**, but for layer 5 PT neurons (n = 560 neurons).

(**H**) As in **E**, but for layer 5 PT neurons.

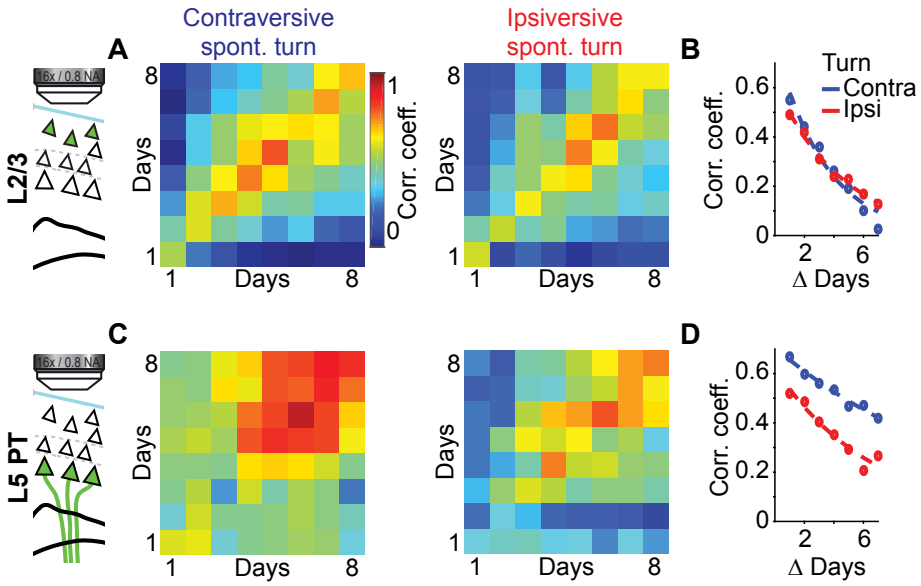

Figure S5. Activity during spontaneous turns is more stable in layer 5 PT over the course of training. Related to Figure 4.

(**A**) Stability of layer 2/3 population activity during contraversive (left) and ipsiversive turns (right). Data of each training day was split into first and second half and mean population vectors to contra- and ipsiversive turns computed from both halves. Shown is the average Pearson's correlation coefficient of the population vector (n = 1154 neurons) computed from the first half of the data (x-axis) with the population vector computed from the second half of the data (y-axis) as a function of days of training. Color indicates Pearson's correlation coefficient.

(**B**) Average Pearson's correlation coefficients of population vectors for contraversive (blue) and ipsiversive (red) turns as a function of the time difference in training days. Dashed lines are exponential fits to the data. Decay time constants are 3.3 and 4.6 days for contra- and ipsiversive turns, respectively.

(**C**) As in **A**, but for layer 5 PT neurons (n = 560 neurons).

(**D**) As in **B**, but for layer 5 PT neurons (n = 560 neurons). Decay time constants are 13.6 and 6.9 days for contra- and ipsiversive turns, respectively. Dashed lines are exponential fits to the data.

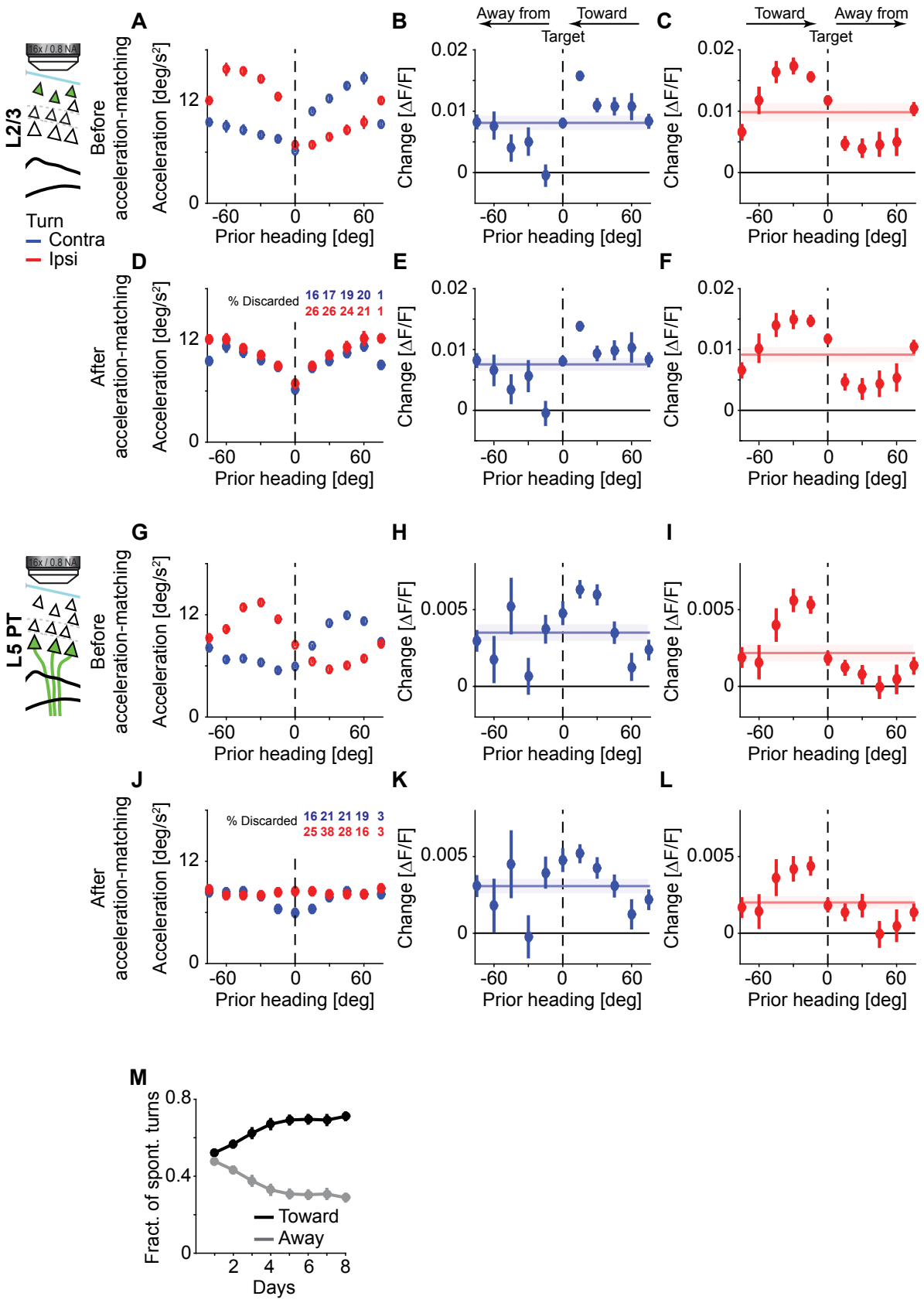
A
B
C
D
E
F
G
H
I
J
K
L
M
16x / 0.8 NA
L2/3
L5 PT
Before acceleration-matching
After acceleration-matching
Turn
Contra
Ipsi
Acceleration [deg/s²]
Change [ΔF/F]
Prior heading [deg]
Away from
Toward
Target
% Discarded
16 17 19 20 1
26 26 24 21 1
16 21 21 19 3
25 38 28 16 3
Fract. of spont. turns
Toward
Away
Days

Figure S6. Acceleration-matching of turns toward and away from target. Related to Figure 5.

(**A**) Average acceleration of the turn binned to heading prior to spontaneous turn onset for contraversive (blue) and ipsiversive (red) turns, before acceleration-matching. Data recorded throughout training (days 1 to 8) were used in this analysis. On average, turns toward the target are executed at higher acceleration than turns away from the target. A prior heading of 0 (dashed line) marks direction of target. Error bars indicate SEM over turns.

(**B**) Average activity of contraversive layer 2/3 neurons (n = 616 neurons) during contraversive spontaneous turns as a function of heading preceding the turn, before acceleration-matching. Data recorded throughout training (days 1 to 8) were pooled. Error bars indicate SEM over turns. Horizontal blue line and shading indicate the average response and SEM over turns. Solid black line marks 0 $\Delta F/F$.

(**C**) As in **B**, but for ipsiversive neurons (n = 538 neurons) and ipsiversive turns.

(**D**) As in **A**, with bins acceleration-matched pairwise around 0 degrees prior heading (see STAR Methods). Numbers at the top indicate the percentage of data that were discarded for each bin pair by the acceleration-matching procedure.

(**E**) As in **B**, but for acceleration-matched contraversive turns.

(**F**) As in **C**, but for acceleration-matched ipsiversive turns.

(**G**) As in **A**, but for layer 5 PT data set.

(**H**) As in **B**, but for contraversive layer 5 PT neurons (n = 229 neurons).

(**I**) As in **C**, but for ipsiversive layer 5 PT neurons (n = 331 neurons).

(**J**) As in **D**, but for layer 5 PT data set.

(**K**) As in **E**, but for contraversive layer 5 PT neurons.

(**L**) As in **F**, but for ipsiversive layer 5 PT neurons.

(**M**) Fraction of spontaneous turns that are taken toward (black) or away (gray) from target as a function of imaging days. Error bars indicate SEM over mice (n = 19 mice).

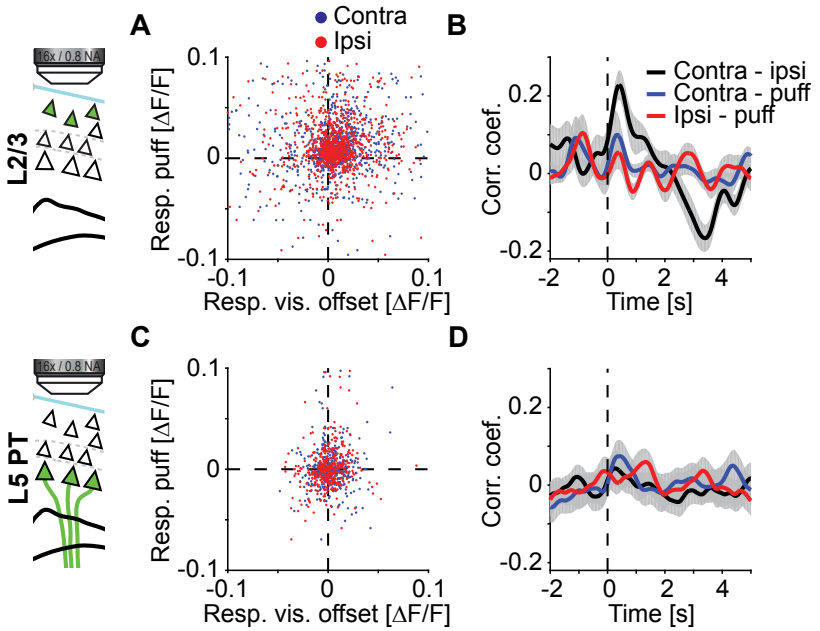

Figure S7. Visual perturbation offset responses do not correlate with air puff responses.

(**A**) Scatter plot of the average visual offset perturbation response recorded throughout training (days 3 to 8) versus the average air puff response for contra- (blue) and ipsiversive (red) layer 2/3 neurons. Each dot represents the response of an individual neuron (n = 973 neurons).

(**B**) Pearson's correlation coefficient of the population vector of layer 2/3 neurons (n = 973 neurons) during air puff stimulus and either contra- (blue) or ipsiversive (red), or contra- and ipsiversive (black) visual offset perturbation-induced turns, respectively, as a function of time around event onset. Gray shading marks an estimate of standard deviation (see STAR Methods).

(**C**) As in **A**, but for layer 5 PT neurons (n = 394 neurons).

(**D**) As in **B**, but for layer 5 PT neurons (n = 394 neurons).

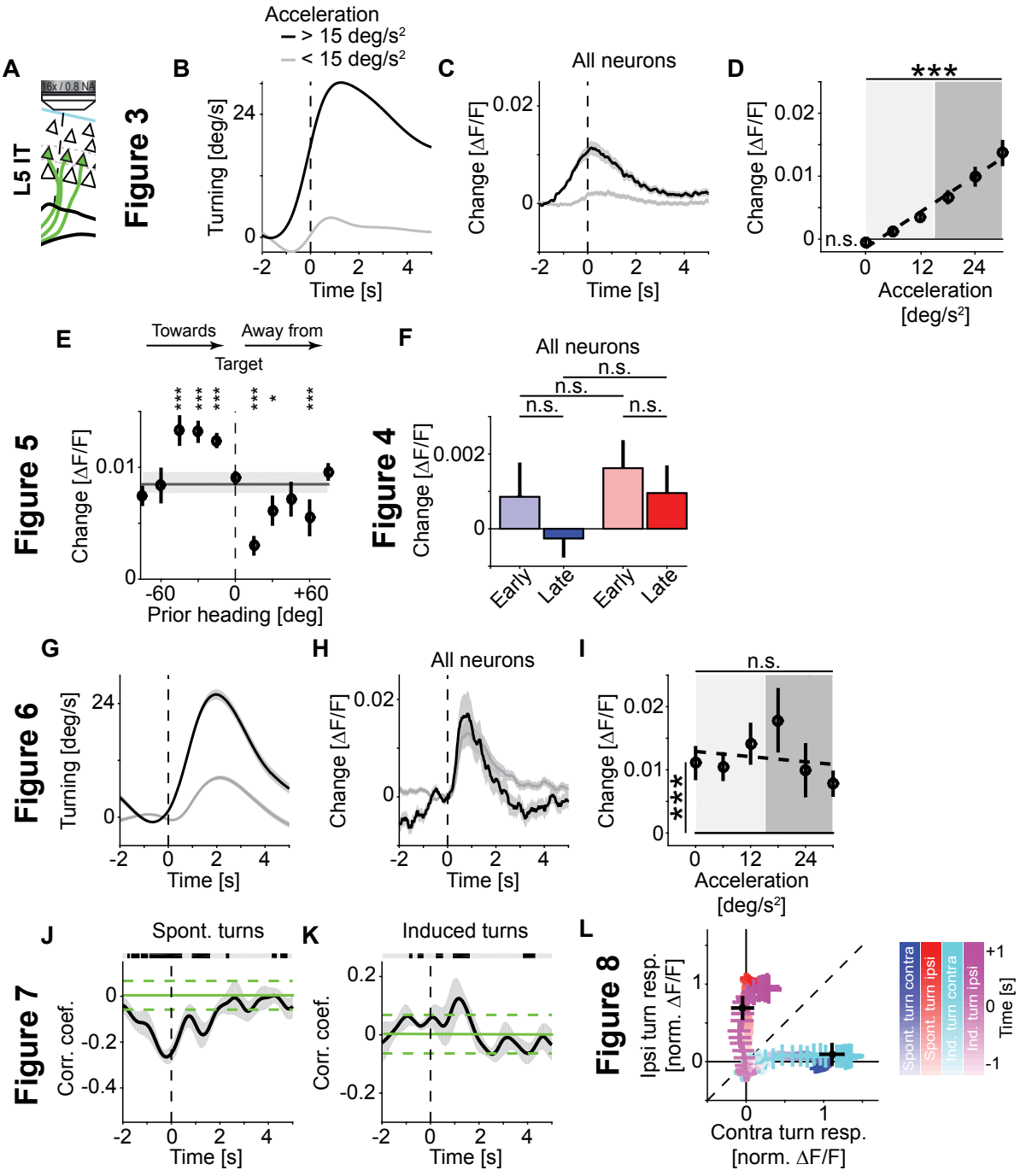
A
16x / 0.8 NA
L5 IT
Figure 3
B
Acceleration
> 15 deg/s²
< 15 deg/s²
Turning [deg/s]
24
0
-2 0 2 4
Time [s]
C
All neurons
Change [ΔF/F]
0.02
0
-2 0 2 4
Time [s]
D
***
Change [ΔF/F]
0.02
0.01
0
n.s.
0 12 24
Acceleration [deg/s²]
E
Towards
Away from
Target
Change [ΔF/F]
0.01
0
-60 0 +60
Prior heading [deg]
Figure 5
F
All neurons
n.s.
n.s.
n.s.
n.s.
Change [ΔF/F]
0.002
0
Early
Late
Early
Late
Figure 4
G
Turning [deg/s]
24
0
-2 0 2 4
Time [s]
H
All neurons
Change [ΔF/F]
0.02
0
-2 0 2 4
Time [s]
I
n.s.
Change [ΔF/F]
0.02
0.01
0
***
0 12 24
Acceleration [deg/s²]
Figure 6
J
Spont. turns
Corr. coef.
0
-0.2
-0.4
-2 0 2 4
Time [s]
K
Induced turns
Corr. coef.
0.2
0
-0.2
-2 0 2 4
Time [s]
Figure 7
L
Ipsi turn resp. [norm. ΔF/F]
1
0
0 1
Contra turn resp. [norm. ΔF/F]
Spont. turn contra
Spont. turn ipsi
Ind. turn contra
Ind. turn ipsi
+1
0
-1
Time [s]
Figure 8

Figure S8. Layer 5 IT neurons exhibit properties intermediate to those observed in layer 2/3 and layer 5 PT neurons.

(**A**) Schematics of the imaging experiments in layer 5 intratelencephalic (IT) projection neurons. To record the activity of layer 5 IT neurons we injected conditional AAV2/1-DIO-EF1α-GCaMP6f into *Tlx3(PL56)-Cre* mice (n = 9 mice).

(**B**) We split all spontaneous turns executed throughout training (days 1 to 8) into bins of high (black line) and low (gray line) acceleration. Shading indicates SEM over turns (number of turns for high acceleration bin: n = 7969; low acceleration bin: n = 8202).

(**C**) Larger turns were associated with higher neuronal activity. Average population activity of layer 5 IT neurons for the turns shown in **B** (n = 308 neurons). Colors as in **B**. Shading indicates SEM over neurons.

(**D**) Average population activity for layer 5 IT neurons as a function of acceleration of the spontaneous turn. Error bars indicate SEM over neurons (n = 308 neurons). Dashed black line is a linear fit to the data. Shading marks bins used for the turning and activity traces in **B** and **C**. ***: $p < 10^{-3}$, $R^2 = 0.06$, n = 308 neurons; linear trend analysis (see STAR Methods). n.s.: not significant, lowest bin is not different from zero; Student's t test.

(**E**) Average activity during spontaneous turns in layer 5 IT neurons as a function of the heading in a window -0.625 s to -0.125 s preceding the turn. Turns executed throughout training (days 1 to 8) were acceleration-matched (see STAR Methods) and binned such that a negative prior heading indicates a turn toward the target and a positive prior heading a turn away from the target. Error bars indicate SEM over turns. Horizontal gray line and shading indicate the average response and SEM over turns. *: $p < 0.05$, ***: $p < 10^{-3}$; Student's t test against the center bin. Bins that are not significant are not marked.

(**F**) Average layer 5 IT responses during contraversive (blue) and ipsiversive (red) turns early (days 1 to 4) and late (days 5 to 8) in training. Responses during neither contraversive nor ipsiversive turns changed with training. Error bars indicate SEM over neurons (n = 308 neurons). n.s.: not significant; paired Student's t test.

(**G**) We split visual offset perturbation-induced turns recorded throughout training (days 3 to 8) into bins of high (black line) and low (gray line) acceleration. Shading indicates SEM over turns (number of turns for high acceleration bin: n = 421; low acceleration bin: n = 1038).

(**H**) Average response in layer 5 IT neurons for the high (black line) and low (gray line) acceleration turns as defined in **G**. Both low and high acceleration turns result in almost identical activation of layer 5 IT neurons (n = 308).

(**I**) Average population response of layer 5 IT neurons as a function of acceleration of the induced turn. Error bars indicate SEM over neurons (n = 308 neurons). Dashed black line is a linear fit to the data. Shading marks bins used for the turning and activity traces in **G** and **H**. ***: $p < 10^{-3}$, Student's t test of first bin versus no response; n.s.: not significant, paired Student's ttest of first vs last bin. We found no evidence of a linear trend ($p = 0.8$, $R^2 = 0.003$, n = 308 neurons; linear trend analysis, see STAR Methods).

(**J**) Pearson's correlation coefficient of the population vector during contraversive and ipsiversive turns as a function of time around turn onset (black line, gray shading marks standard deviation over turns). Horizontal green lines mark mean (solid) and standard deviation (dashed) of random correlation. Horizontal black line marks time bins in which correlation is significantly different from chance (gray indicates bins that are not significant).

(**K**) Same as **J**, but for visual offset perturbation-induced turns.

(**L**) We projected the population vector activity of layer 5 IT neurons onto the plane spanned by the population vector 1 s after turn onset during spontaneous contraversive and spontaneous ipsiversive turns. Origin of the coordinate system is the mean population vector preceding turns. We first projected the population vector during spontaneous contraversive (blue) and spontaneous ipsiversive (red) turns executed throughout training (days 1 to 8) onto this coordinate system. By design projections start at the origin and peak at 1 on their axis. Shading of the maker indicates time relative to turn onset. We then projected the population activity vector during induced contraversive (cyan) and induced ipsiversive turns (magenta) executed during training days 3 to 8 onto the same coordinate system. Black crosses mark the first bin with the first significant change in turning velocity following visual offset perturbation. Error bars indicate SEM over turns. Dashed black line marks line of unity.

SUPPLEMENTAL TABLES

	Total neurons recorded per mouse ± SEM	**Contraversive** neurons per mouse ± SEM	**Ipsiversive** neurons per mouse ± SEM
Layer 2/3 (8 mice)	144 ± 15	77 ± 14	67 ± 15
Layer 5 PT (11 mice)	51 ± 14	21 ± 8	30 ± 9
Layer 5 IT (9 mice)	34 ± 5	15 ± 3	19 ± 3

Table S1. Number of contraversive and ipsiversive neurons per mouse. Related to Figure 3.

Figures	Experiments	Sample size (*genotype*)
1C	Quantification of learning without and with optogenetic inhibition	**Control group (black):** n = 22 mice (3 *vGAT::ChR2(H134R)::EYFP*, 8 *vGAT-Cre* x *ROSA-LSL-tdTom*, 11 *Sim1-Cre(KJ18)*) **Optogenetics group (blue):** n = 12 mice (*vGAT::ChR2(H134R)::EYFP*)
1D	Performance testing without and with optogenetic inhibition	n = 15 mice (*vGAT::ChR2(H134R)::EYFP*)
2A-B, 2E-F	Quantification of turning behavior without optogenetic inhibition	n = 22 mice (3 *vGAT::ChR2(H134R)::EYFP*, 8 *vGAT-Cre* x *ROSA-LSL-tdTom*, 11 *Sim1-Cre(KJ18)*)
2C-D, 2G-H	Quantification of turning behavior with optogenetic inhibition	n = 14 (*vGAT::ChR2(H134R)::EYFP*)
3C-F, 4A-C, 5A, 6A-C, 7A-F, 8A	Quantification of turning related activity in layer 2/3 data set	n = 8 mice (*vGAT-Cre* x *ROSA-LSL-tdTom*) 1154 successively recorded neurons
3G-J, 4D-F, 5B, 6D-F, 7G-L, 8B	Quantification of turning related activity in layer 5 PT data set	n = 11 mice (*Sim1-Cre(KJ18)*), 560 successively recorded neurons
S1C-E	Additional quantification of learning impairment with optogenetic inhibition or chronic ibotenic acid lesions	**Control group (black):** n = 22 mice (3 *vGAT::ChR2(H134R)::EYFP*, 8 *vGAT-Cre* x *ROSA-LSL-tdTom*, 11 *Sim1-Cre(KJ18)*) **Optogenetics group (blue):** n = 12 mice (*vGAT::ChR2(H134R)::EYFP*) **Ibotenic acid group (brown):** n = 5 mice (*C57/BL6*)
S1F	Comparison of performance impairment in expert mice at two different stimulus locations in motor cortex	n = 9 mice (*vGAT::ChR2(H134R)::EYFP)*
S1H	Learning slope comparison without and with optogenetic inhibition	**Optogenetics groups (purple):** n = 3 mice (*vGAT::ChR(H134R)::EYFP*) **Control group (black):** n = 22 mice (3 *vGAT::ChR2(H134R)::EYFP*, 8 *vGAT-Cre* x *ROSA-LSL-tdTom*, 11 *Sim1-Cre(KJ18)*)
S1I	Quantification of learning in wild type mice with optogenetic stimulation	**Control group (black):** n = 22 mice (3 *vGAT::ChR2(H134R)::EYFP*, 8 *vGAT-Cre* x *ROSA-LSL-tdTom*, 11 *Sim1-Cre(KJ18)*) **Optogenetics group (orange):** n = 4 (*C57/Bl6*)

S2A-S2B	Quantification of induced turning behavior with and without chronic optogenetic inhibition	**Laser OFF group (left):** n = 3 (*vGAT::ChR(H134R)::EYFP*) **Laser ON group (right):** n = 12 (*vGAT::ChR(H134R)::EYFP*)
S2C-S2E	Quantification of behavior with and without timed optogenetic inhibition	n = 14 (*vGAT::ChR(H134R)::EYFP*)
S2F-I	Quantification of wild type turning behavior with optogenetic inhibition	n = 6 (*C57/Bl6*)
S3C-E	Comparison of layer 5 PT soma and dendrite activity	**Upper row:** n = 3 mice (*Sim1-Cre(KJ18)*) **Lower row:** n = 8 mice (*Sim1-Cre(KJ18)*)
S4A, S4C-E, S5A-B, S6A-F, S7A-B	Quantification of turning and running related activity in layer 2/3 data set	n = 8 mice (*vGAT-Cre* x *ROSA-LSL-tdTom*) 1154 successively recorded neurons
S4B, S4F-H, S5C-D, S6G-L, S7C-D	Quantification of turning and running related activity in layer 5 PT data set	n = 11 mice (*Sim1-Cre(KJ18)*), 560 successively recorded neurons
S7M	Quantification of learning related change in the number of target-directed turns	n = 19 mice (8 *vGAT-Cre* x *ROSA-LSL-tdTom*, 11 mice (*Sim1-Cre(KJ18)*)
S8	Quantification of main effects in layer 5 IT data set	n = 9 mice (*Tlx3-Cre(PL56)*), 308 successively recorded neurons

Table S2. Experiments and sample size reported in this manuscript. Related to STAR Methods.